DOI: 10.1002/cmdc.201402562

Design and Synthesis of a MAO-B-Selectively Activated Prodrug Based on MPTP: A Mitochondria-Targeting Chemotherapeutic Agent for Treatment of Human Malignant Gliomas

Martyn A. Sharpe,[a] Junyan Han,[a] Alexandra M. Baskin,[b] and David S. Baskin*[a]

Malignant gliomas, including glioblastomas, are extremely difficult to treat. The median survival for glioblastoma patients with optimal therapeutic intervention is 15 months. We developed a novel MAO-B-selectively activated prodrug, *N*,*N*-bis(2-chloroethyl)-2-(1-methyl-1,2,3,6-tetrahydropyridin-4-yl)propanamide (MP-MUS), for the treatment of gliomas based on 1-methyl-4-phenyl-1,2,3,6-tetrahydropyridine (MPTP). The design of neutral MP-MUS involved the use of a seeker molecule capable of binding to mitochondrial MAO-B, which is up-regulated $\geq$fourfold in glioma cells. Once the binding occurs, MP-MUS is converted into a positively charged moiety, P^{+}-MUS, which accumulates inside mitochondria at a theoretical maximal value of 1000:1 gradient. The LD_{50} of MP-MUS against glioma cells is 75 μM, which is two- to threefold more potent than temozolomide, a primary drug for gliomas. Importantly, MP-MUS was found to be selectively toxic toward glioma cells. In the concentration range of 150–180 μM MP-MUS killed 90–95% of glioma cells, but stimulated the growth of normal human astrocytes. Moreover, maturation of MP-MUS is highly dependent on MAO-B, and inhibition of MAO-B activity with selegiline protected human glioma cells from apoptosis.

Introduction

Gliomas, or glial tumors, are the most common primary brain tumors in humans[1] and include a group of neoplasms with distinct histological and genetic features. Among them, glioblastomas (GBMs) and anaplastic astrocytomas are the most aggressive primary malignant tumors, with an annual incidence of 5.3 per 100000, or 17000 new diagnoses per year in the USA.[2] Temozolomide (TMZ) is the primary and most commonly used chemotherapeutic drug for the treatment of gliomas. TMZ has poor therapeutic indices; it kills healthy tissues almost as effectively as tumor tissues.[3,4] Its efficacy is limited, as the median life expectancy for glioma patients after radiation therapy and TMZ treatment is 15 months.[4,5] Therefore, it is highly desirable to develop new antineoplastic drugs for the treatment of malignant gliomas. Herein we describe the use of a prodrug, MP-MUS, based on 1-methyl-4-phenyl-1,2,3,6-tetrahydropyridine (MPTP), which is selectively activated by monoamine oxidase B (MAO-B). Data are presented to demonstrate MP-MUS is two- to threefold more potent against glioma cells than TMZ. Importantly, MP-MUS is selectively activated by glioma cells and accumulates inside gliomal mitochondria, resulting in the selective destruction of cancer cells without causing damage to normal cells.[6] In comparison with TMZ, MP-MUS shows promising features for the treatment of gliomas; to our knowledge, it is the first known example of selective mitochondrial chemotherapy.[7]

Monoamine oxidases (MAOs) are flavoenzymes that are located on the outer mitochondrial membranes. Two MAO isoforms, MAO-A and MAO-B, are found in human body. The two enzymes are differentiated by their tissue distribution and substrate specificity (see review[8]). The specific activity of MAO-B is higher in human brain than in other organs, such as kidney, liver, heart, and lungs.[9] MAO-B/-A ratios are found to be >14 throughout white matter, and between 5.9 and 9.0 in gray matter in human brain tissue,[10] with MAO-B primarily found in non-neuronal cells such as astrocytes and radial glia; it is, however, present in serotonergic neurons.[11] Brain MAOs modulate neurotransmitter levels through oxidative deamination of a number of amines, generating the corresponding aldehydes and hydrogen peroxide.

By measuring MAO oxidation of phenylethylamine in the absence or presence of the MAO-B-specific inhibitor L-deprenyl (selegiline), MAO-B activity was found to be significantly up-regulated in glial tumors relative to control brain tissue or non-glial brain tumors.[12] Immuno-histological studies in our research group have confirmed this observation (unpublished results). We speculate that glioma-targeting prodrugs could be

[a] *Prof. Dr. M. A. Sharpe,[+] Dr. J. Han,[+] Prof. Dr. D. S. Baskin*
Kenneth R. Peak Brain and Pituitary Tumor Center
Department of Neurological Surgery
Neurological Institute, Houston Methodist Hospital
Weill Cornell Medical College of Cornell University
6565 Fannin Street, Houston, TX, 77030 (USA)
E-mail: dbaskin@houstonmethodist.org

[b] *A. M. Baskin*
St. Johns School, 2401 Claremont Lane, Houston, TX, 77019 (USA)

[+] *These authors contributed equally to this work.*

Supporting information for this article is available on the WWW under http://dx.doi.org/10.1002/cmdc.201402562: characterization data for compounds **1**–**3**, MP-Est, and MP-MUS.

developed by using the oxidation capacities of MAO-B. The difference in substrate pocket shape between the two MAO isoforms provides feasibility to develop a prodrug which will be selectively metabolized by MAO-B over MAO-A, resulting in fewer side effects.[13]

Results and Discussion

Design and synthesis of prodrug MP-MUS

We designed the MAO-B-activated prodrug MP-MUS based on a known transformation of a nontoxic compound, MPTP, into the neurotoxin MPP^+ (Figure 1 a). Mice[14] and primates[15] have high levels of MAO-B in brain tissue, and are therefore sensitive to MPTP. Nontoxic MPTP is oxidized by MAO-B or human cytochrome P450 2D6[16] to form MDP^+, which undergoes further oxidation (typically by the mitochondrial quinone pool[17]) to form the neurotoxin MPP^+ (Figure 1 a). MPP^+ is a substrate for the dopamine transporter (DAT), which transports MPP^+ inside dopaminergic neurons. As a lipophilic cation, MPP^+ diffuses across the mitochondrial membrane in a Nernstian fashion,[18,19] and inhibits mitochondrial respiration by interfering with complex I of the electron-transport chain, resulting in neuron damage, selective loss of dopaminergic neurons, and Parkinsonian syndrome.[20] 1-Methyl-1,2,3,6-tetrahydropyridine (MTP) and some of its derivatives, such as MPTP, are known selective MAO-B substrates.[21] These MTP substrates could be oxidized by MAO-B to form pyridinium cations, which accumulate in mitochondria. If covalently conjugated to a cytotoxic DNA-alkylating moiety, specific MTP substrates can act as anti-glioma prodrugs activatable by MAO-B,[22] exhibiting both antitumor activity through alkylation of mitochondria DNA (mtDNA) and low toxicity toward normal tissues.

We chose nitrogen mustard (MUS),[23] a traditional antineoplastic DNA alkylation drug used since 1943, as a prototype drug for conjugation to MTP. This led to our first functional MAO-B-activated prodrug, MP-MUS (Figure 1 b). MTP is the moiety for MAO-B binding, and MUS is the cytotoxic fragment capable of alkylating a wide range of biomolecules, such as DNA. We proposed that MP-MUS should be oxidized by MAO-B to MD^+-MUS, and then further oxidized into the mature drug, P^+-MUS.[24] Lipophilic cations such as MPP^+ preferentially accumulate in the mitochondrial matrix of cells, driven by the mitochondrial membrane potential; it has been demonstrated that in energized mitochondria MPP^+ displays classical Nernstian behavior,[18] and P^+-MUS has been designed to act in the same manner. The steady-state accumulation of P^+-MUS inside mitochondria can be estimated from the Nernst equation [Equations (1) and (2)]:[19]

$$\Delta\Psi = \left(\frac{2.3\,RT}{mF}\right)\log_{10}\left(\frac{[X^{m+}]_{in}}{[X^{m+}]_{out}}\right) \quad (1)$$

$$180\ \text{mV} = 60\log_{10}\left(\frac{[P^+\text{-MUS}]_{in}}{[P^+\text{-MUS}]_{out}}\right) \quad (2)$$

in which $\Delta\Psi$ is mitochondrial membrane potential, R is the gas constant, T is temperature, m is the charge number, and F is the Faraday constant. In glioma cells, which have a mitochondrial membrane potential of ≈180–200 mV,[25] the concentration of $[P^+\text{-MUS}]_{in}$ will be theoretically ≈1000-fold greater than $[P^+\text{-MUS}]_{out}$.

Nitrogen mustards typically attack DNA and other important biomolecules via the highly reactive three-membered aziridinium ring (Supporting Information (SI), Figure S1).[26] However, the presence of an amide in MP-MUS allows the formation of a five-membered dihydrooxazolium ring capable of alkylating mitochondria DNA and inducing apoptosis. (SI Figure S1). Specific accumulation of P^+-MUS in the mitochondria of MAO-B-overexpressing glioma cells, but not in those of normal noncancerous cells, is a function of the mature drug.

Like MPP^+, P^+-MUS could be a substrate for DAT. Therefore, MP-MUS chemotherapy could kill dopaminergic neurons, resulting in Parkinson's disease. To determine whether M^+-MUS is a good substrate for DAT, we conducted modeling studies based on the nortriptyline-inhibited form of the crystal structure of the *Drosophila melanogaster* dopamine transporter (PDB ID: 4M48;[27] SI Figure S2). Modeling studies suggest that P^+-MUS is too large to be a DAT substrate. The DAT transporting channel is like a constraining ring above the sodium ions which bind the amine of a substrate/inhibitor. S422 plays a crucial role in DAT substrate selectivity, as it can block of the movement of large amines through the DAT channel. Therefore, the S422A mutant form, which has a slightly larger constraining ring, has a far wider substrate specificity than the wild-type.[28] In Supporting Information Figures S2 A and S2 B we show a model of the top and side views of substrates, dopamine and MPP^+, along with P^+-MUS and the inhibitor nortriptyline in the 4M48 DAT crystal structure. Unlike dopamine and MPP^+, the dibenzocycloheptene 'parasol' of nortrip-

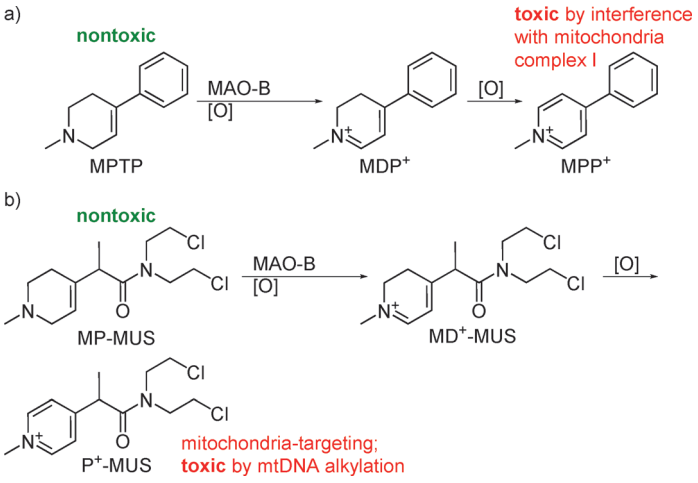

Figure 1. Design of MAO-B-activated prodrug MP-MUS based on MPTP: a) MPTP toxicity mechanism; b) design of the MP-MUS prodrug. MPTP = (1-methyl-4-phenyl-1,2,3,6-tetrahydropyridine; MDP^+ = 1-methyl-4-phenyl-2,3-dihydropyridinium; MPP^+ = 1-methyl-4-phenylpyridinium.

tyline is too wide to go through the DAT annular constraining ring (SI Figure S2C(I)). The chloroethyl 'wings' of P^+-MUS make this compound unlikely to move through this annular ring either, being blocked by S422 (SI Figure S2C(II)). In addition, P^+-MUS is too large to fit into the substrate binding pocket of the 4M48 structure, overlapping with the valine residue that constrains substrate length.

The synthesis of MP-MUS is illustrated in Scheme 1. The Horner–Wadsworth–Emmons reaction of *N*-methylpiperidone with triethyl 2-phosphonopropionate produced the α,β-conjugated ester **1**. Treatment of compound **1** with LDA (THF, −72 °C, 1 h), followed by quenching with NH_4Cl, yielded the critical β,γ-unsaturated ester MP-Est, a racemic compound, in nearly quantitative yield. MP-Est was hydrolyzed (2 equiv 1 N KOH, 2 h, 60 °C) to form acid **2**. Under these harsh hydrolysis conditions, the double bond of MP-Est was not isomerized, as indicated by the ^{1}H NMR spectra of **2** and MP-Est (SI). Carboxylic acid **2** was converted into acid chloride with $SOCl_2$, then joined diethanolamine (1 equiv) to afford crude amide **3**.[20] Finally, the racemic prodrug MP-MUS was synthesized by converting the dihydroxy groups in compound **3** into dichlorine with $SOCl_2$.[20] Direct coupling of compound **2** to diethanolamine via other common coupling reagents, such as DCC or BOP, could not be satisfactorily accomplished probably as a result of the low activity of the carboxylic acid.

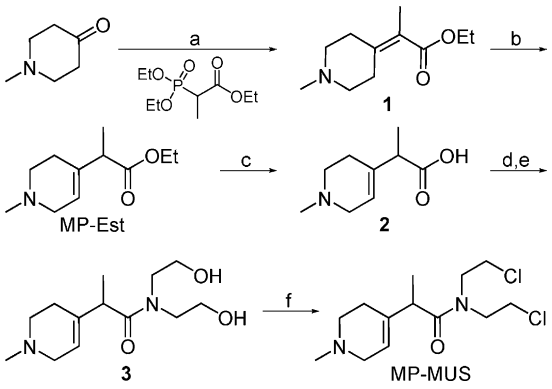

Scheme 1. Synthesis of MP-MUS. *Reagents and conditions*: a) NaH, THF, 20 °C, overnight; b) LDA, THF, −72 °C, 1 h; c) KOH (2 N), H_2O, 60 °C, 2 h; d) $SOCl_2$, 70 °C, 1 h; e) diethanolamine, CH_2Cl_2, 20 °C, 1 h; f) $SOCl_2$, benzene, 80 °C, 5 h. LDA = lithium diisopropylamide; DMF = *N*,*N*′-dimethylformamide.

UV absorbance spectra changes in the reaction of MP-Est with MAO-A/-B

Partially purified recombinant human MAO-A and MAO-B (Sigma–Aldrich; M7316 (150 U mg^{-1}), and M7441 (52 U mg^{-1})) were used to examine the enzyme specificity of MP-MUS and its precursors. Using high chloride buffer to decrease the reactivity of MP-MUS,[29] we attempted to monitor the oxidation of MP-Est and MP-MUS by both MAOs, observing the formation of the oxidation intermediate 1-methyl-2,3-dihydropyridinium and the final oxidation product 1-methyl-pyridinium, which have UV absorbance spectra peaking at ~365 and 292 nm, respectively.[24] MP-Est and MP-MUS (2 mM) were incubated with either MAO-A (14 U mL^{-1}, 94 μg mL^{-1}) or MAO-B (7 U mL^{-1}, 140 μg mL^{-1}) in 1 mL buffer (pH 7.4) containing 50 mM KPi and 100 mM NaCl at 37 °C; UV absorbance spectra were taken every 5 min using a BioTeck Synergy HT spectrophotometer. We observed large light scattering during the incubation of MP-MUS at 2 mM with the partly purified MAOs, but especially with MAO-B, which made UV spectral changes very difficult to interpret. However, we were able to observe the formation of a dihydropyridinium peak centered at 380 nm using 600 μM MP-MUS. No such light-scattering changes were observed using unreactive MP-Est, which produced UV signatures of both expected products. The real-time UV absorbance changes during the oxidation of MP-Est with MAO-A/-B were measured over a period of 45 min. As shown in Figure 2, both enzymes produced a significant amount of the first and final oxidation products MD^+-Est (dihydropyridinium, 365 nm) and P^+-Est (pyridium, 292 nm), respectively (two structures shown in SI Figure S3). The substantially larger absorbance peak exhibited during the MAO-B oxidation than with MAO-A, despite a two-fold higher MAO-A concentration, indicated that oxidation of MP-Est by MAO-B is much faster than by MAO-A.

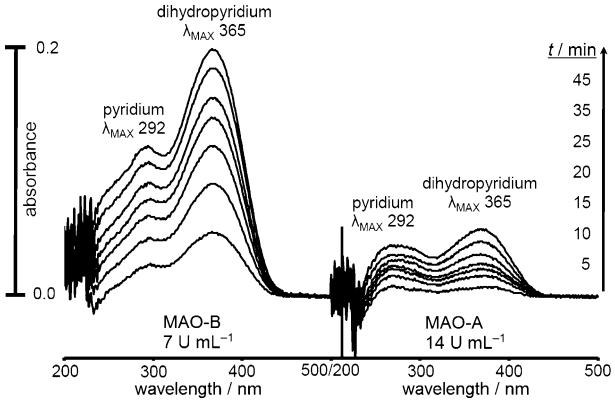

Figure 2. Real-time UV absorbance spectra of the reaction between MAO-B (left, 7 U mL^{-1}) or MAO-A (right, 14 U mL^{-1}) and MP-Est (2.0 mM) over the course of 45 min.

Kinetics of MAO-A/-B on substrates tyramine, MP-Est, and MP-MUS

The kinetics of MP-MUS oxidation catalyzed by MAO-A and -B were measured by monitoring the rate of hydrogen peroxide generation with the Amplex Red/horse radish peroxidase (HRP) system.[30] H_2O_2 is one of the key products generated during MAO-catalyzed oxidative deamination of a number of primary amines in the brain.[31] The rates of H_2O_2 generation during the oxidation of substrates tyramine (Tyr), MP-Est, and MP-MUS by either MAO-A or MAO-B are shown in Figure 3. Tyr is a known nonselective substrate;[32] therefore, it is expected that the H_2O_2 generation rate for Tyr metabolism by MAO-A is similar to that by MAO-B. This is exactly what we measured, as the V_{max} of MAO-A is the same as that of MAO-B, indicating both en-

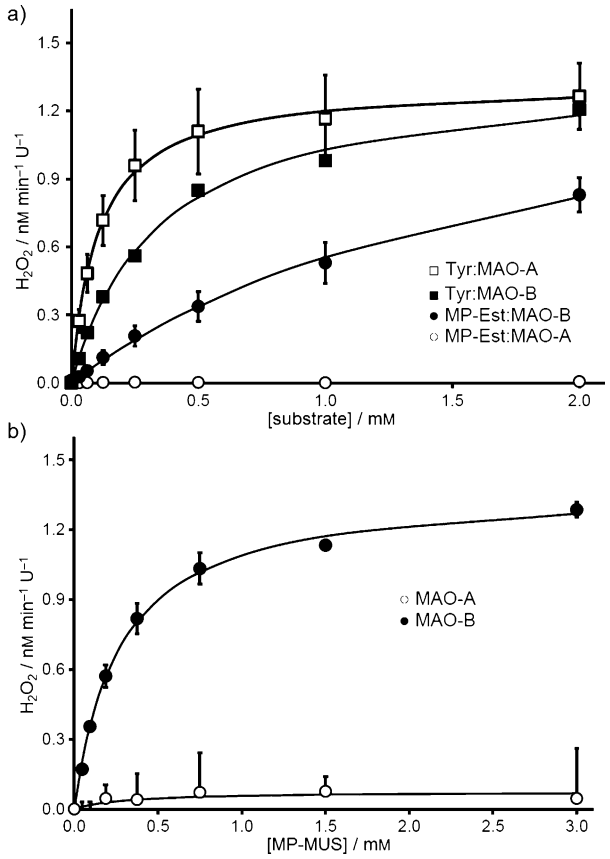

Figure 3. Rate of H_2O_2 production by MAO-A/-B activities with substrates a) Tyr and MP-Est and b) MP-MUS, at the indicated concentration ranges. [Concentration series are different between panels a) and b).] Data are the mean ± SD of $n = 3$ experiments.

zymes can oxidize Tyr efficiently. The K_M for MAO-A is slightly smaller than for MAO-B; therefore, MAO-A oxidizes Tyr faster than MAO-B. In addition, Figure 3a shows MP-Est to have been rapidly oxidized by MAO-B, but very slowly by MAO-A. Finally, the data presented in Figure 3b demonstrate that MP-MUS is a remarkably good substrate for MAO-B, but a very poor MAO-A substrate. Pre-incubating MAO-B with the inhibitor selegiline caused a block in MAO-B-catalyzed H_2O_2 generation by MP-MUS and other substrates.

The data shown in Figure 3 and those of other kinetic studies were fitted to the Michaelis–Menten equation, and the parameters, such as K_M, V_{max}, and V_{max}/K_M, were calculated and are presented in Table 1. V_{max}/K_M is a measure of how efficiently MAOs convert a substrate into the corresponding oxidization products. As for the substrate Tyr, V_{max}/K_M values for MAO-A and MAO-B are 12.1 and $3.97\times10^{-6}\,U^{-1}\,s^{-1}$ respectively, indicating both enzymes oxidized Tyr efficiently, but MAO-A did this threefold faster than MAO-B. The MAO-B-specific substrates BA and 4-FBA were only oxidized by MAO-B, and no activity was observed with MAO-A.[33] MAO-B oxidized MP-MUS with V_{max}/K_M at $5.15\times10^{-6}\,U^{-1}\,s^{-1}$, a slightly higher rate than for Tyr. It is clear that MP-MUS is poorly oxidized by MAO-A, with V_{max}/K_M at $1.7\times10^{-7}\,U^{-1}\,s^{-1}$. The V_{max}/K_M ratio of MAO-B/-A is $30.3\times10^{-6}\,U^{-1}\,s^{-1}$, indicating that MP-MUS is metabolized at a rate

Table 1. Parameters for the kinetics of oxidation of tyramine (Tyr), benzylamine (BA), 4-fluorobenzylamine (4-FBA), MP-Est, and MP-MUS by MAO-A/MAO-B.

Substrate	MAO-A[a]			MAO-B[a]			B/A[b]
	K_M	V_{max}	V_{max}/K_M	K_M	V_{max}	V_{max}/K_M	
Tyr	0.11	1.33	12.1	0.35	1.39	3.97	0.33
BA	–	< 0.01	–	0.12	2.3	19.2	–
4-FBA	–	< 0.01	–	0.12	2.4	20	–
MP-Est	–	< 0.01	–	1.86	1.58	0.85	–
MP-MUS	0.3	0.05	0.17	0.27	1.39	5.15	30.3

[a] Units: K_M [mM], V_{max} [nM U^{-1} s^{-1}], V_{max}/K_M [10^{-6} U^{-1} s^{-1}]. [b] Ratio of V_{max}/K_M for MAO-B/MAO-A.

30-fold faster by MAO-B than MAO-A. The much more efficient oxidation of MP-MUS by MAO-B than MAO-A suggests that MP-MUS preferentially gains access to the larger substrate cavity of MAO-B,[34] resulting in a MAO-B-selective substrate.[35]

Cytotoxicity of MP-MUS on human glioma cells and normal human astrocytes

Finally, we investigated the cytotoxic effect of MP-MUS on human primary glioma cells and normal human astrocytes (NHAs), the latter of which are the most abundant normal glial cells in human brains. MP-MUS showed distinct toxic effects toward glioma cells and NHAs. The toxic effects of dose escalation of MP-MUS on glioma cells with 48 h treatment are shown in Figure 4a. The number of viable cells decreased with increasing MP-MUS concentration. If [MP-MUS] is > 150 μM, < 13% glioma cells remain alive. The LD_{50} of MP-MUS against glioma cells is ~75 μM. In comparison with halting cell proliferation, MP-MUS caused the opposite pattern of dead cell fractions (blue trace in Figure 4a). TMZ is the most commonly used chemotherapeutic drug for the clinical treatment of glioma, and has an LD_{50} value of ~150–200 μM.[36] MP-MUS is about two- to threefold more potent against glioma cells than TMZ. The effects of dose escalation of MP-MUS on NHAs are shown in Figure 4b. MP-MUS showed not only an absence of cytotoxicity toward normal human astrocytes up to 180 μM, but stimulated cell growth, possibly due to the generation of mitogen H_2O_2 in the oxidation process.[37] At an MP-MUS concentration of 210 μM, some 86% NHAs survived, whereas the same treatment caused 95% gliomal cell death. The distinct cytotoxicity effects of MP-MUS on human primary glioma cells and not NHAs were further validated by fluorescence microscopy. As shown in Figure 4c (I–III), treatment of GBMs with MP-MUS (90 μM) induced apoptosis, as indicated by shrunken cytoplasm, condensed nuclei, and disrupted mitochondria. At 210 μM MP-MUS, there were no indications of morphological changes related to apoptosis in NHAs, whereas the gliomal cells are clearly in a pathological state (Figure 4c (VI–IV)).

To determine whether the differential toxic effects of MP-MUS on glioma cells and NHAs are caused by the difference in intracellular MAO-B levels, we first measured the concentration of MAO-B in both cells via measurement of fluorescence intensity of Alexa Fluor 488-labeled anti-MAO-B antibody. The data

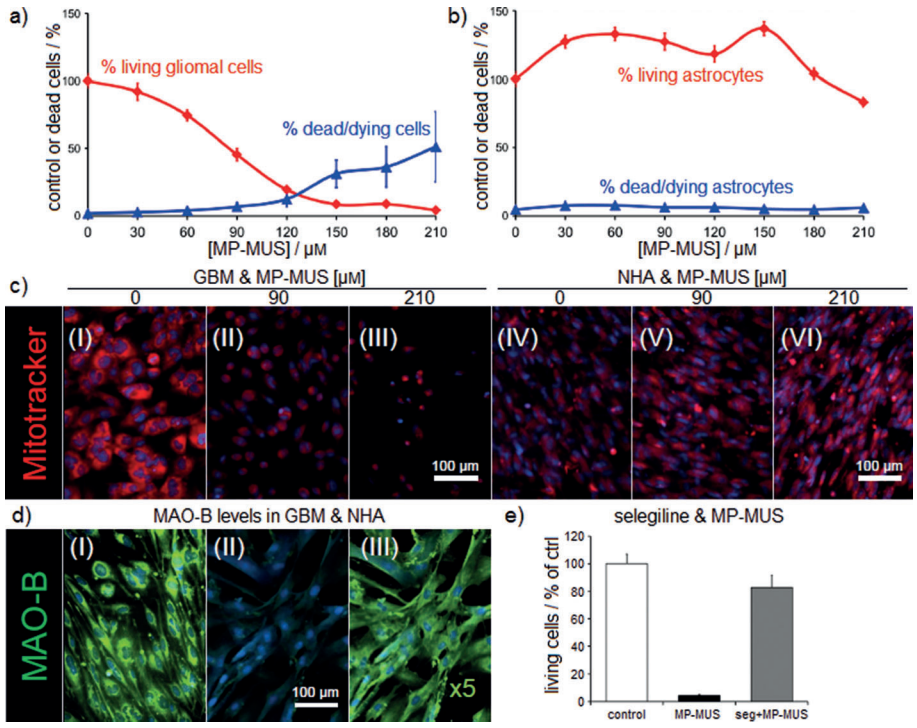

Figure 4. Studies of MAO-B-dependent cytotoxicity of MP-MUS. The cytotoxicity effects of MP-MUS (0–210 μM, 48 h) on a) glioma cells (GBMs) and b) normal human astrocytes (NHAs). Data are the mean ± SEM of $n = 8$ experiments. c) Fluorescence images of human glioma cells (I, II, III) and NHAs (VI, V, IV) after treatment with MP-MUS at the indicated concentrations. Red and blue are signals from MitoTracker Red FM and nucleus marker Hoechst 33342, respectively. d) Fluorescence signals of MAO-B antibody in I) glioma cells and II) NHAs; III) 5× green signals in (II). e) Effects of the MAO-B inhibitor selegiline (10 μM) on the toxicity of MP-MUS (210 μM) against glioma cells for 48 h; data are the mean ± SEM of $n = 8$ experiments.

presented in Figure 4d suggest that NHAs expressed ≈5-fold less MAO-B than glioma cells, which is in good agreement with reported data.[12] To further study the MAO-B-dependent toxicity of MP-MUS, we exposed human primary glioma cells to selegiline prior to treatment with MP-MUS at 210 μM. Without selegiline, MP-MUS was found to be highly toxic, and only 5% of cells survived a 48 h incubation (middle column in Figure 4e), whereas 83% of glioma cells were viable with selegiline pre-treatment. Incubation of cells with the MAO-A inhibitor clorgyline had little effect on the toxicity of MP-MUS in a parallel experiment (data not shown). Our results demonstrate that cells lacking high MAO-B activity, such as a patient's noncancerous cells/tissues, have significantly lower sensitivity to MP-MUS toxicity.

Conclusions

In summary, we designed, synthesized, and tested the first MAO-B-selectively activated prodrug MP-MUS based on MPTP, which exerts its anticancer action inside the mitochondria of brain cancer cells. To our knowledge, this is the first example of selective mitochondrial chemotherapy. The maturation of the prodrug MP-MUS is like the mechanism by which nontoxic MPTP is converted into neurotoxin MPP^+. The maturation of MP-MUS is established first by the oxidation by MAO-B to form 1-methyl-2,3-dihydropyridinium MD^+-MUS, and further oxidation to generate the mature drug pyridinium P^+-MUS, which alkylates mtDNA and induces cell death. The enzyme kinetics measured by monitoring the rate of H_2O_2 generation showed that MAO-B oxidized MP-MUS to form the toxic mature drug 30 times as efficient as MAO-A. This indicates that MP-MUS can be selectively converted into toxic P^+-MUS by MAO-B. We demonstrated that MP-MUS is capable of selectively killing primary human glioma cells with an LD_{50} value of 75 μM at 48 h, while causing little damage to NHA. The relatively high doses of MP-MUS are needed to kill primary human glioma possibly because of the non-enzymatic hydrolysis of the mustard groups, with the chlorines being replaced by hydroxy groups, generating nontoxic alcohols. Nevertheless, our MP-MUS showed greater potency against brain glioma cells than TMZ, which has an LD_{50} value in the range of 150–200 μM.[36] In addition, the specific MAO-B inhibitor selegiline was shown to protect glioma cells from MP-MUS, indicating the action of our prodrug toxicity is highly contingent on the activity of MAO-B. Importantly, we demonstrated that MP-MUS is selectively toxic toward glioma cells, but not toxic to NHAs, which have lower MAO-B expression levels.

Treatment of gliomas with our new drug MP-MUS in animal studies has demonstrated promising results, and will be reported soon. We envision that MP-MUS, and similar bifunctional mitochondrial-targeting MAO-B-activated prodrugs, will be a promising clinical strategy for the treatment of human gliomas.

Experimental Section

Reagents and materials: Tested compounds including tyramine (Tyr) and selegiline were purchased from Sigma–Aldrich with purity >95% and were used directly without further purification. MP-Est was synthesized with >95% purity, as determined by a high-pressure liquid chromatography (HPLC) system (Phenomenex Luna C-18(2), 250 mm × 10 mm, 5 μm) mobile phase: A = H_2O, B = MeOH; flow rate: 4.0 mL min^{-1}; gradient: 10→82% B in 9.0 min. MAO-A and MAO-B were obtained from Sigma (M7316, batch SLBJ7414V, M7441, batch SLBJ6906V). MP-MUS was synthesized with purity >95% as determined by HPLC (Phenomenex Luna C-18(2), 250 mm × 4.6 mm, 5 μm) mobile phase: A = H_2O (0.5% TFA), B = CH_3CN (0.5% TFA); flow rate: 1.0 mL min^{-1}; gradient: 10→50% B in

10.0 min. MP-MUS is a fragile compound and decomposes slowly in solvents; therefore, it must be stored under nitrogen at −80 °C. MitoTracker Red FM (MT, M22425) and Hoechst 33342 for DNA were purchased from Life Technologies (Invitrogen/Molecular Probes, Eugene, OR, USA).

Synthesis of compounds 1, 2, 3, MP-Est, and MP-MUS. All reagents and solvents were purchased from Sigma–Aldrich. All syntheses were performed under an atmosphere of nitrogen unless indicated otherwise. ^{1}H and ^{13}C NMR spectra were obtained with a Bruker 500/600 MHz and 125 MHz magnetic resonance spectrometer, respectively. Solvent peaks of $CDCl_3$ at 7.26 and 77.1 ppm were used as internal standards for ^{1}H and ^{13}C NMR, respectively. Data for ^{1}H NMR spectra are reported as follows: chemical shift, multiplicity (s = singlet, d = doublet, t = triplet, q = quartet, b = broad, m = multiplet), coupling constants, and number of protons. Low-resolution mass spectra (LRMS) were recorded on a quadrupole spectrometer using electrospray ionization (ESI). Analytical thin-layer chromatography was conducted on glass sheets coated with silica gel 60 F_{254}. Flash chromatography was performed on regular grade silica gel (60 Å, Fisher Scientific).

E**thyl 2-(1-methylpiperidin-4-ylidene)propanoate (1)**: NaH (3.83 g, 0.096 mol) was added slowly to a solution of ethyl 2-diethoxyphosphorylpropanoate (28 mL, 0.13 mol) in anhydrous THF (87 mL) in a 250-mL flask kept in an ice bath. The mixture was stirred at 0 °C for 15 min, and then 1-methylpiperidin-4-one (10 mL, 0.087 mol) was added dropwise to the solution. The solution was slowly warmed to room temperature, and stirring continued overnight. The reaction was quenched by the addition of H_2O (50 mL), and the product was extracted with EtOAc (3×35 mL). The combined organic solvent was washed with H_2O (1×20 mL) and brine (1× 20 mL), dried over anhydrous Na_2SO_4, and finally removed under reduced pressure. The crude residue was purified by regular silica gel chromatography eluting with MeOH/CH_2Cl_2 (1:10) to yield the desired product as light-yellow oil (10.5 g) in 61% yield. R_f = 0.23 (MeOH/CH_2Cl_2 = 1:10); ^{1}H NMR ($CDCl_3$, 500 MHz): δ = 4.17 (q, J = 7.0 Hz, 2H), 2.64–2.62 (m, 2H), 2.45–2.40 (m, 4H), 2.38–2.36 (m, 2H), 2.26 (s, 3H), 1.85 (s, 3H), 1.28 ppm (t, J = 7.0 Hz, 3H); ^{13}C NMR ($CDCl_3$, 150 MHz): δ = 170.0, 143.5, 121.3, 60.3, 56.5, 56.1, 45.8, 31.3, 30.4, 22.4, 15.1, 14.3 ppm; LRMS calcd for $C_{11}H_{20}NO_2^+$ $[M+H^+]^+$ 198.2, found 198.2.

Ethyl 2-(1-methyl-1,2,3,6-tetrahydropyridin-4-yl)propanoate (MP-Est): Compound **1** (119 mg, 0.604 mmol) was dissolved in anhydrous THF (1.0 mL) and the solution was merged in a −72 °C bath (dry ice in EtOH). A solution of LDA (0.91 mL, 2 M) was then added dropwise to the former solution. The final solution was stirred at −72 °C for 1 h, and then the reaction was quenched with saturated NH_4Cl. The product was extracted from H_2O with EtOAc (3×20 mL). The combined organic phase was washed with deionized H_2O, brine, and then dried over anhydrous Na_2SO_4. The salt was removed by filtration, and the solvent was removed under reduced pressure. The residue was purified by chromatography on silica gel eluting with EtOAc (3% Et_3N) to yield the desired product as a yellow oil (117 mg, 99% yield). ^{1}H NMR ($CDCl_3$, 500 MHz): δ = 5.53 (br s, 1H), 4.11 (q, J = 7.0 Hz, 2H), 3.08 (q, J = 7.0 Hz, 1H), 3.03 (br s, 2H), 2.65–2.60 (m, 2H), 2.38 (s 3H), 2.25 (br d, J = 16.5 Hz, 1H), 2.16 (br d, J = 16.5 Hz, 1H), 1.25 (d, J = 7.0 Hz, 3H), 1.23 ppm (t, J = 7.0 Hz, 3H); ^{13}C NMR ($CDCl_3$, 125 MHz): δ = 174.2, 135.0, 120.3, 60.6, 53.6, 51.4, 46.1, 44.7, 26.4, 15.1, 14.3 ppm; LRMS calcd for $C_{11}H_{20}NO_2^+$ $[M+H^+]^+$ 198.2, found 198.1.

2-(1-Methyl-1,2,3,6-tetrahydropyridin-4-yl)propanoic acid (2): MP-Est (27 mg, 0.137 mmol) was dissolved in KOH (0.137 mL, 2 M). The mixture was stirred at 60 °C for 2 h. The solution was carefully neutralized to pH 6 (HCl, 1 M), and the solvent was removed under reduced pressure. The crude compound was further purified by chromatography on regular silica gel eluting with EtOH/NH_4OH (5:1 *v/v*) to yield the desired product as a gelatinous white solid (23 mg, 100% yield). R_f = 0.23 (EtOH/NH_4OH 5:1 *v/v*); ^{1}H NMR (CD_3OD, 500 MHz): δ = 5.55 (br s, 1H), 3.70 (br s, 2H), 3.35–3.33 (m, J = 6.0 Hz, 1H), 3.03 (q, J = 7.0 Hz, 2H), 2.89 (s, 3H), 2.54–2.51 (m, 1H), 2.45–2.42 (m, 1H), 1.24 ppm (d, J = 7.0 Hz, 3H); ^{13}C NMR ($CDCl_3$, 125 MHz): δ = 179.5, 137.8, 114.1, 51.8, 50.4, 48.5, 41.5, 24.0, 15.0 ppm; LRMS calcd for $C_9H_{16}NO_2^+$ $[M+H^+]^+$ 170.2, found 170.1.

***N*,*N*-Bis(2-hydroxyethyl)-2-(1-methyl-1,2,3,6-tetrahydropyridin-4-yl)propanamide (3)**: The mixture of compound **2** (30 mg, 0.178 mmol) and $SOCl_2$ (0.30 mL) were stirred at 70 °C for 1 h. The solvent was removed under reduced pressure. Then the residue was dissolved in anhydrous CH_2Cl_2, and diethanolamine (17 μL, 0.178 mmol) was added, followed by anhydrous pyridine (0.1 mL). The reaction mixture was stirred at room temperature for 1 h. The solvent was removed under reduced pressure. The crude compound was used directly for the next step without further purification; LRMS calcd for $C_{13}H_{25}N_2O_3^+$ $[M+H^+]^+$ 257.2, found 257.1.

***N*,*N*-Bis(2-chloroethyl)-2-(1-methyl-1,2,3,6-tetrahydropyridin-4-yl)propanamide (MP-MUS)**: Compound **3** (22 mg, 0.086 mmol) and $SOCl_2$ (0.1 mL) were stirred at 70 °C for 3 h. The solvent was removed under reduced pressure. Then the residue was purified by flash chromatography on basic alumina eluting with CH_2Cl_2/MeOH (30:1 *v/v*) to yield the desired product as a light-yellow solid (16 mg, 65% yield). R_f = 0.2 (CH_2Cl_2/MeOH 30:1 *v/v*); ^{1}H NMR ($CDCl_3$, 600 MHz): δ = 5.56 (br s, 1H), 3.86 (q, J = 7.2 Hz, 1H), 3.80 (t, J = 6.0 Hz, 4H), 3.70–3.67 (m, 3H), 3.54 (br s, 2H), 3.43–3.36 (m, 1H), 3.16 (t, J = 6.0 Hz, 4H), 2.84 (s, 3H), 1.30 ppm (d, J = 7.2 Hz, 3H); LRMS calcd for $C_{13}H_{23}N_2Cl_2O^+$ $[M+H^+]^+$ 293.1, 295.1, found 293.0, 295.0.

4-(1-(Bis(2-chloroethyl)amino)-1-oxopropan-2-yl)-1-methyl-1,2,3,6-tetrahydropyridinium chloride (MP-MUS·HCl): The neutral form MP-MUS that was prepared by following the protocol above was dissolved in anhydrous EtOH (2 M HCl, 3 equiv). The removal of solvent under reduced pressure gave the desired product as a white solid.

Primary human GBM: A glioblastoma (GBM) tumor was taken at the time of excision and given the laboratory ID of BT150. It was chopped with a scalpel and then homogenized with a 5-mL pipette. The cells were grown in Dulbecco's modified Eagle's medium (DMEM) with fetal bovine serum (FBS, 20%), 1× GlutaMax-I, sodium pyruvate (1 mM), penicillin (100 U mL^{-1}), and streptomycin (100 μg mL^{-1}). BT150 cells are spontaneously immortal and were frozen at fourth passage and used between seventh and ninth passages. Glioma cells were grown to achieve confluency in either Costar 96-well plates (Corning, NYC, NY, USA) or 16-well Lab-Tek slide chambers (Nalge Nunc International, Rochester, NY, USA). Low-passage human glioma primary culture, BT150, was used in all the in vitro data presented, although we have used a number of other low-passage primary glioblastoma cultures to confirm results.

Normal human astrocytes (NHAs): NHAs were obtained from Lonza (Walkersville, MD, USA) and subjected to their recommendations for growth. NHAs were grown to confluency in astrocyte cell basal medium supplemented with 3% FBS, 1% glutamine, 0.1% insulin, 0.1% rhEGF, 0.1% GA-1000, and 0.25% ascorbic acid (from Clonetics™ AGM™ BulletKit™ (CC-3186)) in 96-well plates or in 16-well Lab-Tek slide chambers in a total volume of 250 μL.

Measurements of H_2O_2 generation with Amplex Red: For Tyr and MP-Est: substrates, Amplex Red (150 μM), and HRP (3 U mL^{-1}) were incubated with MAOs (1 U mL^{-1}) in pH 7.4 buffer (50 mM KPi, 100 mM NaCl) at 37 °C for 15 min in 96-well format (75 μL volume per well). The formation of fluorescent resorufin (λ_{ex} 500–560 nm, λ_{em} 565–625 nm) was measured in a BioTeck Synergy HT spectrophotometer. The maximal signal generated from Amplex Red (150 nmol mL^{-1}) was established by the addition of H_2O_2 (1 mM) to each well at the end of the assay period.

For MP-MUS: We found that MP-MUS was a potent inhibitor of HRP, and therefore was eliminated from the 15 min incubation period of dye, MAO, and MP-MUS. HRP (3U mL^{-1}) was added to the mix at the end of 15 min, just prior to fluorescence measurement.

Fluorescence microscopy: Images were captured using a Nikon Eclipse TE2000-E at 4× or 20× magnification using a CoolSnap ES digital camera system (Roper Scientific) containing a CCD-1300-Y/HS 1392×1040 imaging array that is cooled by Peltier. Images were recorded and analyzed using Nikon NIS-Elements software (Elements 3.22.11). All images were saved as JPEG2000 files using Nikon NIS-Elements. The emission of goat anti-rabbit IgG antibody labeled with Alexa Fluor 488 was collected through the FITC (λ_{ex} 450–490 nm, λ_{em} 500–550 nm). The fluorescence of MTR was obtained through the Texas Red filter set (λ_{ex} 510–550 nm, λ_{em} 573–648 nm), whereas Hoechst 33342 was taken via the DAPI filter set (λ_{ex} 325–375 nm, λ_{em} 435–485 nm).

Cell viability and cell death assay: MP-MUS·HCl was added to a DMSO solution to make a stock solution (7.5 mM). GBM cells or NHAs were treated with MP-MUS (0, 30, 60, 90, 120, 150, 180, 210 μM), and all wells received the same 8-μL DMSO vehicle volume (total volume of 250 μL). After treatment, cells were grown in the presence of all effectors (37 °C, 5% CO_2). At $t=47$ h, cells were incubated with Hoechst 33342 (10 μM) in the presence and absence of MitoTracker Red FM (1 μM, M22425) for 1 h and then were fixed with ice-cold 4% paraformaldehyde (PFA). We conducted cell counts in center field at 20× magnification, so that there was an average of 150 cells per image and between one and eight dead or dying cells visualized in the same field. Dead/dying cells were identified as having condensed nuclei with signal intensities over threefold that of the median cell nuclei. Dividing cells identified by paired and brightly labeled nuclei were counted as two living cells.

Measurement of MAO-B levels in glioma cells and NHAs: Glioma cells were permeabilized with 0.1% Triton X-100 in PBS and treated with Dako protein blocking solution (X0909, Dako North America, Carpinteria, CA, USA). Rabbit anti-MAO-B (clone EPR7103, Cat #ab125010, Abcam, Cambridge, MA, USA) was used to identify MAO-B and was diluted 1:500 using Dako antibody diluent (S3022). Goat anti-rabbit IgG antibody labeled with Alexa Fluor 488 (A11034) was used to visualize for primary rabbit antibody to MAO-B.

Acknowledgements

This work was supported by the Donna and Kenneth R. Peak Foundation, the Kenneth R. Peak Brain and Pituitary Center at Houston Methodist Hospital, the Taub Foundation, the Blanche Green Estate Fund of the Pauline Sterne Wolff Memorial Foundation, the Verelan Foundation, the Houston Methodist Hospital Foundation, the American Brain Tumor Association, and many patients and families who have been impacted by the devastating effects of brain tumors and central nervous system disease. We thank the MD Anderson Cancer Center for use of their NMR facility.

Keywords: DNA damage · gliomas · MAO-B · MPTP · prodrugs

[1] A. Omuro, L. M. DeAngelis, *JAMA J. Am. Med. Assoc.* **2013**, *310*, 1842–1850.
[2] T. A. Dolecek, J. M. Propp, N. E. Stroup, C. Kruchko, *J. Neuro-Oncol.* **2012**, *14*, v1–49.
[3] J. P. Mannas, D. D. Lightner, S. R. Defrates, T. Pittman, J. L. Villano, *J. Clin. Neurosci.* **2014**, *21*, 121–123.
[4] Y. P. Ramirez, J. L. Weatherbee, R. T. Wheelhouse, A. H. Ross, *Pharmaceuticals* **2013**, *6*, 1475–1506.
[5] M. Preusser, S. de Ribaupierre, A. Wohrer, S. C. Erridge, M. Hegi, M. Weller, R. Stupp, *Ann. Neurol.* **2011**, *70*, 9–21.
[6] Y. Singh, M. Palombo, P. J. Sinko, *Curr. Med. Chem.* **2008**, *15*, 1802–1826.
[7] L. Galluzzi, N. Larochette, N. Zamzami, G. Kroemer, *Oncogene* **2006**, *25*, 4812–4830.
[8] J. C. Shih, K. Chen, M. J. Ridd, *Annu. Rev. Neurosci.* **1999**, *22*, 197–217.
[9] a) N. M. Freedman, E. Mishani, Y. Krausz, J. Weininger, H. Lester, E. Blaugrund, D. Ehrlich, R. Chisin, *J. Nucl. Med.* **2005**, *46*, 1618–1624; b) J. Saura, E. Nadal, B. van den Berg, M. Vila, J. A. Bombi, N. Mahy, *Life Sci.* **1996**, *59*, 1341–1349.
[10] J. Tong, J. H. Meyer, Y. Furukawa, I. Boileau, L. J. Chang, A. A. Wilson, S. Houle, S. J. Kish, *J. Cereb. Blood Flow Metab.* **2013**, *33*, 863–871.
[11] a) K. N. Westlund, R. M. Denney, R. M. Rose, C. W. Abell, *J. Neurosci.* **1988**, *25*, 439–456; b) K. N. Westlund, R. M. Denney, L. M. Kochersperger, R. M. Rose, C. W. Abell, *Science* **1985**, *230*, 181–183; c) P. Levitt, J. E. Pintar, X. O. Breakefield, *Proc. Natl. Acad. Sci. USA* **1982**, *79*, 6385–6389.
[12] A. M. Gabilondo, C. Hostalot, J. M. Garibi, J. J. Meana, L. F. Callado, *Neurochem. Int.* **2008**, *52*, 230–234.
[13] J. P. M. Finberg, *Pharmacol. Ther.* **2014**, *143*, 133–152.
[14] G. E. Meredith, D. J. Rademacher, *J. Parkinsons Dis.* **2011**, *1*, 19–33.
[15] G. Porras, Q. Li, E. Bezard, *Cold Spring Harbor Perspect. Med.* **2012**, *2*, a009308.
[16] P. Bajpai, M. C. Sangar, S. Singh, W. Tang, S. Bansal, G. Chowdhury, Q. Cheng, J.-K. Fang, M. V. Martin, F. P. Guengerich, N. G. Avadhani, *J. Biol. Chem.* **2013**, *288*, 4436–4451.
[17] H. Shi, N. Noguchi, Y. Xu, E. Niki, *FEBS Lett.* **1999**, *461*, 196–200.
[18] G. P. Davey, K. F. Tipton, M. P. Murphy, *Biochem. J.* **1992**, *288*, 439–443.
[19] D. G. Nicholls, S. J. Ferguson, *Bioenergetics 2*, Academic Press Ltd., London, **1992**, P. 59.
[20] Y. Watanabe, T. Himeda, T. Araki, *Med. Sci. Monit.* **2005**, *11*, RA17–RA23.
[21] H. Rollema, E. A. Johnson, R. G. Booth, P. Caldera, P. Lampen, S. K. Youngster, A. J. Trevor, N. Naiman, N. Castagnoli, *J. Med. Chem.* **1990**, *33*, 2221–2230.
[22] Y.-X. Wang, N. Castagnoli, Jr., *Bioorg. Med. Chem.* **1997**, *5*, 1321–1325.
[23] V. T. DeVita, Jr., E. Chu, *Cancer Res.* **2008**, *68*, 8643–8653.
[24] R. R. Fritz, C. W. Abell, N. T. Patel, W. Gessner, A. Brossi, *FEBS Lett.* **1985**, *186*, 224–228.
[25] a) X. Yan, Y. Zhou, S. Liu, *Theranostics* **2012**, *2*, 988–998; b) S. Salvioli, A. Ardizzoni, C. Franceschi, A. Cossarizza, *FEBS Lett.* **1997**, *411*, 77–82; c) A. Cossarizza, M. Baccaranicontri, G. Kalashnikova, C. Franceschi, *Biochem. Biophys. Res. Commun.* **1993**, *197*, 40–45.
[26] A. Polavarapu, J. A. Stillabower, S. G. W. Stubblefield, W. M. Taylor, M.-H. Baik, *J. Org. Chem.* **2012**, *77*, 5914–5921.
[27] A. Penmatsa, K. H. Wang, E. Gouaux, *Nature* **2013**, *503*, 85–90.
[28] T. Beuming, J. Kniazeff, M. L. Bergmann, L. Shi, L. Gracia, K. Raniszewska, A. H. Newman, J. A. Javitch, H. Weinstein, U. Gether, C. J. Loland, *Nat. Neurosci.* **2008**, *11*, 780–789.
[29] E. Watson, P. Dea, K. K. Chan, *J. Pharm. Sci.* **1985**, *74*, 1283–1292.
[30] M. J. Zhou, Z. J. Diwu, N. PanchukVoloshina, R. P. Haugland, *Anal. Biochem.* **1997**, *253*, 162–168.
[31] M. B. H. Youdim, E. Heldman, H. B. Pollard, P. Fleming, E. McHugh, *Neuroscience* **1986**, *19*, 1311–1318.
[32] L. B. Pearce, J. A. Roth, *Arch. Biochem. Biophys.* **1983**, *224*, 464–472.
[33] C. H. Williams, *Biochem Pharmacol* **1974**, *23*, 615–628; A. K. Tan, R. R. Ramsay, *Biochemistry* **1993**, *32*, 2137–2143.

[34] C. Binda, M. Li, F. Hubalek, N. Restelli, D. E. Edmondson, A. Mattevi, *Proc. Natl. Acad. Sci. USA* **2003**, *100*, 9750 – 9755.

[35] a) C. Binda, F. Hubalek, M. Li, Y. Herzig, J. Sterling, D. E. Edmondson, A. Mattevi, *J. Med. Chem.* **2004**, *47*, 1767 – 1774; b) G. Engberg, T. Elebring, H. Nissbrandt, *J. Pharmacol. Exp. Ther.* **1991**, *259*, 841 – 847; c) J. R. Miller, D. E. Edmondson, *Biochemistry* **1999**, *38*, 13670 – 13683; d) L. De Colibus, M. Li, C. Binda, A. Lustig, D. E. Edmondson, A. Mattevi, *Proc. Natl. Acad. Sci. USA* **2005**, *102*, 12684 – 12689.

[36] M. Taspinar, S. Ilgaz, M. Ozdemir, T. Ozkan, D. Oztuna, H. Canpinar, J. A. Rey, A. Sunguroglu, J. S. Castresana, H. C. Ugur, *Tumor Biol.* **2013**, *34*, 1935 – 1947.

[37] A. Jekabsone, P. K. Mander, A. Tickler, M. Sharpe, G. C. Brown, *J. Neuroinflammation* **2006**, *3*, 24.

Received: December 26, 2014
Published online on ■■ ■■, 0000

Specificity is key: We developed a MAO-B-activated prodrug, MP-MUS, for the treatment of brain gliomas. MP-MUS is nontoxic, and can be selectively oxidized by MAO-B, which is overexpressed in glioma cells, to form toxic P^+-MUS. P^+-MUS translocates inside mitochondria passively and alkylates fragile mitochondrial DNA, leading to specific apoptosis of glioma cells, but not normal cells.

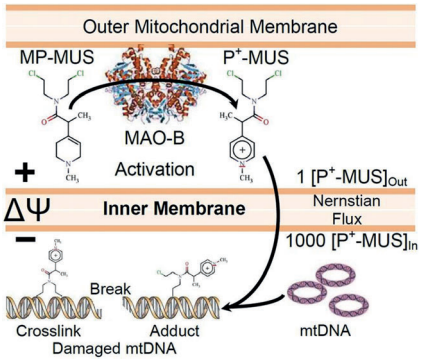

*M. A. Sharpe, J. Han, A. M. Baskin, D. S. Baskin**

■■ – ■■

Design and Synthesis of a MAO-B-Selectively Activated Prodrug Based on MPTP: A Mitochondria-Targeting Chemotherapeutic Agent for Treatment of Human Malignant Gliomas